

Localization of Waves without Bistability: Worms in Nematic Electroconvection

Hermann Riecke

Department of Engineering Sciences and Applied Mathematics
Northwestern University, Evanston, IL 60208, USA

Glen D. Granzow

Department of Mathematics, Idaho State University, Pocatello, ID USA

A general localization mechanism for waves in dissipative systems is identified that does not require the bistability of the basic state and the nonlinear plane-wave state. The mechanism explains the two-dimensional localized wave structures ('worms') that recently have been observed in experiments on electroconvection in nematic liquid crystals where the transition to extended waves is *supercritical*. The mechanism accounts for the propagation direction of the worms and certain aspects of their interaction. The dynamics of the localized waves can be steady or irregular.

submitted February 9, 1998

A striking feature observed in a number of pattern-forming systems with large aspect ratio is the spontaneous localization or confinement of the pattern to a small part of the system although the system is translationally invariant. Presumably the best studied structures of that type are the quasi-one-dimensional pulses of traveling waves that have been found in convection in binary mixtures (e.g. [1]). They have been described theoretically as perturbed solitons (e.g. [2,3]) and as bound pairs of fronts [4,5]. Other quasi-one-dimensional localized structures have been found in Taylor vortex flow [6,7], directional solidification [8], cellular flames [9], and in models for parametrically driven waves [10].

In two dimensions localization appears to be harder to obtain; investigations of binary mixture convection have only led to long-lived, but eventually unstable wave pulses [11]. Only recently have truly stable two-dimensional localized structures been found in parametrically driven surface waves in granular media and in a highly viscous fluid [12]. In most systems the localized structures arise in a regime of bistability. In such situations they can often be considered as a pair of fronts that are bound to each other by dispersion [4], an additional mode [5], or non-adiabatic effects [13–16].

Very recently [17] a two-dimensional localized wave-state has been found in a system in which the transition to the extended waves is *supercritical*, i.e. in which there exist no fronts connecting the basic and the nonlinear state. This rules out the mechanisms of localization mentioned above. Thus, previous efforts to explain these states turn out to be insufficient [15] and the origin of localization has remained quite puzzling. The experiments have been performed in electroconvection of nematic liquid crystals and due to their appearance the new localized states have been called 'worms'.

In this paper we discuss a general mechanism that can lead to localization even if the bifurcation to the extended waves is supercritical. It is based on the presence of an additional, weakly damped field that is advected by the waves and that in turn affects their growth rate. The mechanism explains the shape of the worms, their direction of propagation and certain aspects of their interaction.

Before the theoretical model is introduced a number of features of the experimentally observed worms need to be discussed. Due to the preferred direction associated with the liquid crystal the system has axial anisotropy. In the regime in question convection arises in the form of waves that travel at a fixed angle relative to the axis of anisotropy. Due to reflection symmetry there are four such directions of propagation (left- and right-zig, and left- and right-zag) as indicated in fig.1. The worms consist either of a combination of the left-traveling waves or of the right-traveling waves.

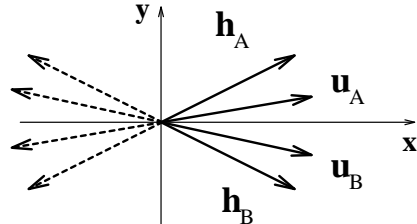


FIG. 1. Sketch of the orientation of the group velocities $\mathbf{u}_{\mathbf{A},\mathbf{B}}$ and of the directions of advection $\mathbf{h}_{\mathbf{A},\mathbf{B}}$ (cf. (1- 3) below).

According to recent calculations the transition to extended waves is supercritical in this regime [18]. This is consistent with the experiments, where for larger conductivity of the liquid crystal extended chaotic waves are observed to arise supercritically and no indication of a change to subcritical behavior of these waves is seen [17]. Nevertheless, the worms arise already at parameter values at which the state without convection is stable [19]. In the x -direction the worms are quite long and their length appears to be somewhat variable. In the y -direction, however, they are very narrow and their width is fixed. Unless perturbed, the worms travel only in the x -direction. In that direction the envelope of the worm has a characteristic shape: it rises rapidly to its maximum at one end and decays slowly over the length of the worm. The worm travels toward the end with the large

amplitude (its ‘head’).

The worms occur very close to threshold and the bifurcation to the extended traveling waves is supercritical [18]. Therefore a set of coupled complex Ginzburg-Landau equations is considered. Since in a given developed worm a single set of zig- and zag-waves is observed [17] we consider only these two waves.

Within the Ginzburg-Landau equations no sustained waves are possible below threshold since all nonlinear terms are damping. We extend therefore these equations introduce an additional, weakly damped mode. The motivation for this mode arises from previous work in the context of binary-mixture convection where it was found by one of the authors that pulses of traveling waves can arise even for a supercritical bifurcation if the waves advect a mode that feeds back into their growth rate [20]. In addition, the weak-electrolyte model, which agrees quantitatively with the experiments with respect to the linear properties [21], suggests that a charge-carrier mode becomes slow in the regime in which worms appear [18].

A minimal model for the advection of a scalar mode by zig- and zag-waves is given by

$$\partial_t A = -\mathbf{u}_A \cdot \nabla A + \mu A + b_x \partial_x^2 A + b_y \partial_y^2 A + 2a \partial_{xy}^2 A \quad (1)$$

$$+ fCA - c|A|^2 A - g|B|^2 A,$$

$$\partial_t B = -\mathbf{u}_B \cdot \nabla B + \mu B + b_x \partial_x^2 B + b_y \partial_y^2 B - 2a \partial_{xy}^2 B \quad (2)$$

$$+ fCB - c|B|^2 B - g|A|^2 B,$$

$$\partial_t C = \delta \partial_x^2 C - \alpha C + \mathbf{h}_A \cdot \nabla |A|^2 + \mathbf{h}_B \cdot \nabla |B|^2. \quad (3)$$

The equations for the complex wave amplitudes A and B are the usual complex Ginzburg-Landau equations for oblique waves [22]. The equation for the scalar mode C is obtained by considering the currents $\mathbf{j}_A \equiv \mathbf{h}_A |A|^2$ and $\mathbf{j}_B \equiv \mathbf{h}_B |B|^2$ that are due to the advection by the respective waves. In addition, damping and diffusion of the mode C is allowed. In the following we first focus on the effect of C and will mostly consider the dispersionless case in which all coefficients are real.

Eqs.(1-3) are solved numerically using a pseudospectral code with an integrating-factor/Runge-Kutta time-stepping scheme. Fig.2 shows a worm solution obtained in this way. For illustration purposes the top part shows the real part of the quantity $Ae^{i\mathbf{q}_A \cdot \mathbf{r}} + Be^{i\mathbf{q}_B \cdot \mathbf{r}}$ which gives an indication of how this solution would appear in experiments. The mode C is shown in the bottom part. As in the experiment the convective amplitude is large at one end of the worm (‘head’) and decays slowly towards the other end. In agreement with the experiments, the worm propagates toward their head.

To understand how this localized solution can arise already below the threshold $\mu = 0$ although the transition to extended waves is supercritical, two one-dimensional reductions of (1-3) are considered. The long and narrow shape of the worms suggests that the localization mechanisms along and transverse to the worm differ from each other. If one ignores the x -dependence, (1-3) reduce to two equations describing standing waves coupled to C

and the worm is replaced by a stationary pulse of standing waves. Such a solution is shown in fig.3. It exists because the C -mode enhances the growth rate in the center of the pulse and keeps the two components A and B together. Since the currents generating C vanish if $|A| = |B|$, the pulse can only exist if the two traveling-wave components are shifted with respect to each other. The shift is due to the group velocity in the y -direction. Thus, the worm disappears in a saddle-node bifurcation when the group velocity is reduced below a certain value. The standing-wave pulse is stable since the production of C increases with the shift between A and B .

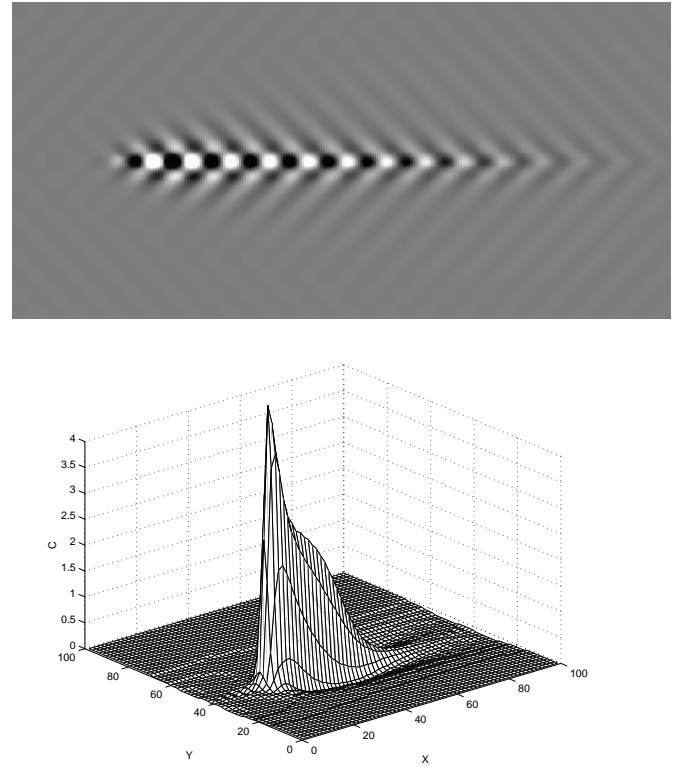


FIG. 2. Numerically determined worm-solution of (1-3) for $\mathbf{u}_A = (0.05, 0.75)$, $\mu = -0.025$, $b_x = b_y = 1$, $a = 0$, $c = 1$, $g = 0.5$, $f = 1$, $\alpha = -0.02$, $\delta = 0.7$, $\mathbf{h}_A = (1, 1)$. a) gray-scale plot of $Ae^{i\mathbf{q}_A \cdot \mathbf{r}} + Be^{i\mathbf{q}_B \cdot \mathbf{r}}$. b) mode C . Note the depression of C along the sides and the back of the worm. The worm travels to the left (toward its ‘head’).

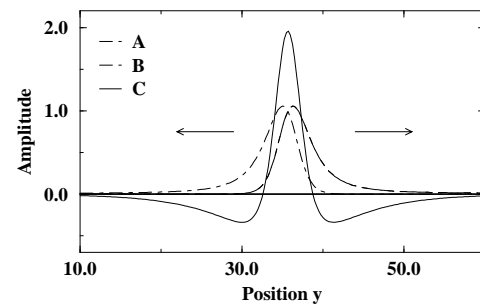


FIG. 3. Standing-wave pulse in one dimension (y -direction). Parameter values corresponding to fig.2.

For the understanding of the stability of the worm solution in fig.2 it is crucial to note that the standing-wave pulse shown in fig.3 arises in a *subcritical bifurcation* although the bifurcation to the extended standing (or traveling) waves is *supercritical*. Thus, the standing-wave pulse can exist already for $\mu < 0$ and can coexist with the basic state $A = B = C = 0$.

The standing-wave pulse can be considered as a building block for the worm: in terms of a one-dimensional reduction along the x -direction the worm can be seen as a pair of fronts connecting the basic state with the *coexisting standing-wave-pulse state*. For stability these two fronts have to exhibit a repulsive interaction. With respect to the x -direction the zig and the zag making up the worms are waves traveling in the same direction. Based on results for traveling-wave pulses [4,5,23] it is therefore expected that the fronts can interact i) *via* the wavenumber [4], which is driven by the dispersive terms, and ii) *via* the additional mode C [5,23].

If the interaction *via C* dominates, a simple connection between the stability of the traveling-wave pulse (here, the worm) and its direction of propagation emerges [5]. As shown in fig.2b there is a large peak of C at the head and a shallow depression of C at the tail. Since positive (negative) C enhances (reduces) the local growth rate of the convective mode both fronts are pushed to the left by C . If the worm travels towards its head, the depression at the trailing front will be reduced by the remnants of the positive peak ahead of it. This is not the case for the leading peak. Thus, the trailing front is pushed less to the left than the leading front amounting to a repulsive interaction. For the traveling-wave pulses this interaction has been determined previously in the limit of weak diffusion δ and damping α and for widely separated fronts [5].

For the present case of fronts in the standing-wave amplitude the corresponding calculation would be considerably more involved. We expect, however, that the same qualitative picture holds. This would imply that the worm is stable if it travels towards its head and unstable otherwise [5]. Indeed the experimentally observed worms travel towards their head. It should be noted that sufficiently strong dispersion can lead to additional stabilization of the worms [23].

When increasing $\mu < 0$ the width of the worm and the maximal value of C remain essentially unchanged, but the worm grows in length. Consequently, the spatial integral $\mathcal{N} = \int |A|^2 dx dy$, which corresponds to a kind of Nusselt number, increases smoothly except for a very small jump in \mathcal{N} at the saddle-node bifurcation in which the worm first appears. In a sufficiently large system, when the threshold $\mu = 0$ is surpassed a sequence of transitions to more than a single worm occurs. When the worms become long enough to span the whole sys-

tem they loose their pronounced head structure and C becomes independent of x .

In the experiments the worms exhibit a typical spacing in the y -direction which decreases with increasing applied voltage. To investigate this aspect within (1-3), the temporal evolution starting from random initial conditions is followed. Fig.4a gives the y -position of the emerging worms as a function of time for $\mu = 0.05$. Fig.4b shows the C -field of the worms at the final time of the run. As in the experiment, the worms approach roughly a typical distance in the y -direction and almost travel on ‘tracks’. When μ is increased the number of ‘tracks’ is found to increase. Fig.4b also demonstrates that the localization mechanism in the y -direction is much stronger than that in the x -direction: while all worms have essentially the same width they vary substantially in their length. This is expected since the localization in the x -direction is achieved *via* the interaction of fronts, which is very weak and decays exponentially in space. Thus, the timescales over which the worms reach their final length is much longer and perturbations from other worms affect the length more strongly than the width.

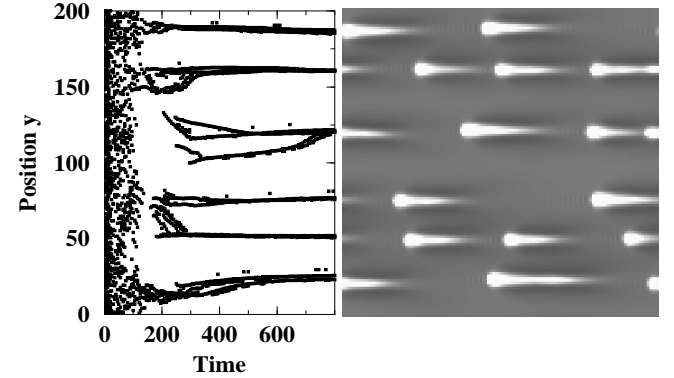


FIG. 4. Formation of worms from random initial conditions. Parameters as in fig.2 except for $\mu = 0.05$ and $\mathbf{u}_A = (0.75, 0.75)$. a) y -location of the maxima in C as a function of time. b) C -field for $t = 800$.

So far the waves have been taken dispersionless. In the experiments it is found that with increasing conductivity the worm regime crosses over to a regime characterized by bursts in the convective amplitude, i.e. patches or blobs of large amplitude appear and disappear in an irregular fashion, and finally a regime of extended convection exhibiting spatio-temporal chaos of patches of zigs, zags, and rectangles is reached [17]. This suggests that dispersion becomes increasingly important along this path in parameter space and indeed the imaginary parts of the coefficients in the Ginzburg-Landau equations for A and B (with C eliminated) increase in this direction [18].

Fig.5 shows the result of a run with intermediate values of the imaginary coefficients. The values have been chosen with some guidance from [18]. In this regime the worms turn out to be unstable and start to travel not only in the x -direction but also in the y -direction. The

motion in the y -direction is driven by imbalances between the amplitudes of the zig- and the zag-component which lead to enhanced advection of C towards one or the other lateral sides of the worm. In addition, the amplitude of the worms grows and decays as indicated by the size of the symbols marking the y -position in fig.5. These strong variations in the amplitude may be related to the bursting seen in the experiments.

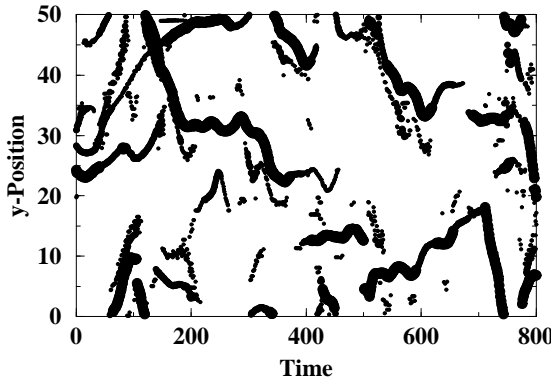


FIG. 5. Unsteady motion of worms. y -location as a function of time for $\mathbf{u}_A = (0.05, 0.05)$, $\mu = 0.05$, $b_x = b_y = 1 - 0.35i$, $a = 0$, $c = 1 + 0.5i$, $g = 0.5 + 0.9i$, $f = 1$, $\alpha = -0.05$, $\delta = 0.4$, $\mathbf{h}_A = (1, 1)$. The size of the symbols indicates the height of the maximum of C .

In conclusion, we have introduced an extension to the complex Ginzburg-Landau equations for zig- and zag-waves that leads in a simple way to localized, worm-like solutions although the bifurcation to extended waves is supercritical. The localization mechanisms differ in the x - and the y -direction: while the worm is spatially homoclinic in the y -direction, i.e. there is only the basic state as a fixed point and the standing-wave pulse represents an excursion from it, it is heteroclinic in the x -direction, i.e. it connects the basic state with a nonlinear periodic solution - the standing-wave pulse - *via* two fronts. Within this framework the worms travel towards their end with larger amplitude, in agreement with experimental observations. The observed typical spacing between the worms in the y -direction is interpreted as the distance over which the advected field C suppresses convection. If one assumes that the damping of the additional mode increases with the conductivity the presented model captures qualitatively the experimentally observed change from steady worms to extended spatio-temporal chaos *via* an irregular bursting as the conductivity is increased. Extended spatio-temporal chaos is obtained when the damping is large and the additional mode can be eliminated [24].

The localization presented here is similar in spirit to that found in parity-breaking bifurcations. There the localized structures are drift waves embedded in a stationary, spatially periodic state (rather than an unpatterned state) [6,8,9] and the additional field is the wavenumber of the underlying pattern [25].

HR grateful acknowledges discussions with L. Kramer,

M. Treiber, Y. Tu, G. Ahlers, and M. Dennin. L. Kramer and M. Treiber kindly made their results available prior to publication. This research has been supported by DOE under grant DE-FG02-92ER14303.

-
- [1] D. Bensimon, P. Kolodner, and C. Surko, *J. Fluid Mech.* **217**, 441 (1990); P. Kolodner, *Phys. Rev. E* **50**, 2731 (1994); J. Niemela, G. Ahlers, and D. Cannell, *Phys. Rev. Lett.* **64**, 1365 (1990); W. Barten, M. Lücke, M. Kamps, and R. Schmitz, *Phys. Rev. E* **51**, 5662 (1995).
 - [2] O. Thual and S. Fauve, *J. Phys. (Paris)* **49**, 1829 (1988).
 - [3] H. Riecke, *Physica D* **92**, 69 (1996).
 - [4] B. Malomed and A. Nepomnyashchy, *Phys. Rev. A* **42**, 6009 (1990); V. Hakim and Y. Pomeau, *Eur. J. Mech. B Suppl* **10**, 137 (1991).
 - [5] H. Herrero and H. Riecke, *Physica D* **85**, 79 (1995).
 - [6] R. Wiener and D. McAlister, *Phys. Rev. Lett.* **69**, 2915 (1992).
 - [7] A. Groisman and V. Steinberg, *Phys. Rev. Lett.* **78**, 1460 (1997).
 - [8] A. Simon, J. Bechhoefer, and A. Libchaber, *Phys. Rev. Lett.* **61**, 2574 (1988).
 - [9] A. Bayliss, B. Matkowsky, and H. Riecke, *Physica D* **74**, 1 (1994).
 - [10] G. Granzow and H. Riecke, *Phys. Rev. Lett.* **77**, 2451 (1996); D. Raitt and H. Riecke, *Phys. Rev. E* **55**, 5448 (1997).
 - [11] K. Lerman, E. Bodenschatz, D. Cannell, and G. Ahlers, *Phys. Rev. Lett.* **70**, 3572 (1993).
 - [12] P. Umbanhowar, F. Melo, and H. Swinney, *Nature* **382**, 793 (1996); O. Lioubashevski, H. Arbell, and J. Fineberg, *Phys. Rev. Lett.* **76**, 3959 (1996).
 - [13] D. Bensimon, B. Shraiman, and V. Croquette, *Phys. Rev. A* **38**, 5461 (1988).
 - [14] H. Sakaguchi and H. Brand, *Physica D* **97**, 274 (1996); H. Sakaguchi and H. Brand, *Europhys. Lett.* **38**, 341 (1997).
 - [15] Y. Tu, *Phys. Rev. E* **56**, R3765 (1997).
 - [16] C. Crawford and H. Riecke, in preparation (1998).
 - [17] M. Dennin, G. Ahlers, and D. Cannell, *Science* **272**, 388 (1996); M. Dennin, G. Ahlers, and D. Cannell, *Phys. Rev. Lett.* **77**, 2475 (1996); M. Dennin, D. Cannell and G. Ahlers, *Phys. Rev. E* **57**, 638 (1998).
 - [18] M. Treiber and L. Kramer, *Phys. Rev. E* (submitted).
 - [19] U. Bisang and G. Ahlers, preprint (1998).
 - [20] H. Riecke, *Physica D* **61**, 253 (1992).
 - [21] M. Dennin *et al.*, *Phys. Rev. Lett.* **76**, 319 (1996).
 - [22] H. Riecke and L. Kramer, preprint (1998).
 - [23] H. Riecke and W.-J. Rappel, *Phys. Rev. Lett.* **75**, 4035 (1995).
 - [24] M. Treiber, H. Riecke, and L. Kramer, unpublished .
 - [25] H. Riecke and H.-G. Paap, *Phys. Rev. A* **45**, 8605 (1992); B. Caroli, C. Caroli, and S. Fauve, *J. Phys. I (Paris)* **2**, 281 (1992).